Published in final edited form as:
J Bone Miner Res. 2011 September ; 26(9): 2151–2160. doi:10.1002/jbmr.425.

Connexin43 Deficiency Reduces the Sensitivity of Cortical Bone to the Effects of Muscle Paralysis[1]

Susan K. Grimston[1], **Daniel B. Goldberg**[1], **Marcus Watkins**[1], **Michael D. Brodt**[2], **Matthew J. Silva**[2], and **Roberto Civitelli**[1,2]

Daniel B. Goldberg: Daniel.goldberg@marquette.edu; Michael D. Brodt: brodtm@wustl.edu; Matthew J. Silva: silvam@wustl.edu; Roberto Civitelli: rcivitel@dom.wustl.edu

[1] Division of Bone and Mineral Disease, Department of Internal Medicine, Washington University School of Medicine, St. Louis, MO, USA

[2] Department of Orthopaedic Surgery, Washington University School of Medicine, St. Louis, MO, USA

Abstract

We have previously shown that the effect of mechanical loading on bone is partly dependent on connexin43 (Cx43). To determine whether Cx43 is also involved in the effect of mechanical unloading, we have used botulinum toxin A (BtxA) to induce reversible muscle paralysis in mice with a conditional deletion of the Cx43 gene in osteoblasts and osteocytes (cKO). BtxA injection in hind limb muscles of wild type (WT) mice resulted in significant muscle atrophy and rapid loss of trabecular bone. Bone loss reached a nadir of about 40% at 3 weeks post-injection, followed by a slow recovery. A similar degree of trabecular bone loss was observed in cKO mice. By contrast, BtxA injection in WT mice significantly increased marrow area and endocortical osteoclast number, and decreased cortical thickness and bone strength. These changes did not occur in cKO mice, whose marrow area is larger, osteoclast number higher, and cortical thickness and bone strength lower relative to WT mice in basal conditions. Changes in cortical structure occurring in WT mice had not recovered 19 weeks after BtxA injection, despite correction of the early osteoclast activation and a modest increase in periosteal bone formation. Thus, BtxA-induced muscle paralysis leads to rapid loss of trabecular bone and to changes in structural and biomechanical properties of cortical bone, neither of which are fully reversed after 19 weeks. Osteoblast/osteocyte Cx43 is involved in the adaptive responses to skeletal unloading selectively in the cortical bone, via modulation of osteoclastogenesis on the endocortical surface.

Keywords

Connexin43; mechanical load; bone morphology

[1]Presented in part at the 31st annual meeting of the American Society for Bone and Mineral Research, Denver, CO, September 2009 and at the 56th annual meeting of the Orthopaedic Research Society, New Orleans, LA, March, 2010.

Address all correspondence and reprint requests to: Susan K. Grimston, Ph.D., Division of Bone and Mineral Diseases, Washington University in St. Louis, 660 Euclid- Campus Box 8301, St. Louis, MO. 63110, Phone: (314) 454-8431, Fax: (314) 454-5325, Sgrimsto@dom.wustl.edu.

CONFLICTS OF INTEREST

Roberto Civitelli has a Material Transfer Agreement with Zealand Pharma, Glostrup, Denmark, for the use of gap junction modifying peptides, but receives no honoraria or research funds from Zealand. He receives consultant fees from Novartis and Amgen, grant support from Eli-Lilly and Pfizer; and own stock of Eli-Lilly, Merck and Amgen. None of the other authors have financial conflicts of interest.

INTRODUCTION

Gap junctions are intercellular channels providing aqueous continuity between cells. Gap junctions in bone are primarily formed by connexin43 (Cx43). The importance of Cx43 for the skeletal system is underscored by the ossification defects in mice with inactivation of the Cx43 gene (*Gja1*) (1), and by the skeletal malformations present in the human disease oculodentodigital dysplasia, a condition linked to loss of function mutations of *Gja1* (2–4). We have recently demonstrated that mice with a conditional ablation of *Gja1* in osteoblasts and osteocytes have low bone mass and show an attenuated response to the anabolic effect of PTH (5) and to anabolic mechanical stimulation (6). Notably, cortical thickness is decreased in the diaphyses of long bones of these animals, a morphology similar to aging bone (7,8) and bones in disuse (9,10), raising the possibility that the bone structure of *Gja1* deficient mice may represent an appropriate adaptation to their lower bone mass, or a failure to properly adapt to normal ambulatory loads.

To garner further insights into the role of Cx43 in skeletal mechano-responsiveness, we have applied a model of skeletal physical unloading by inducing temporary muscle paralysis using botulinum toxin A (BtxA) to mice with a conditional osteoblast/osteocyte specific *Gja1* deletion. BtxA injection in hind limb muscles causes a reversible muscle paralysis associated with rapid and profound bone loss, followed by slower recovery of bone mass as muscle function resumes (11–15). Thus, this approach allows the study of not only the effects of mechanical disuse on bone, but also the potential for bone recovery with the gradual resumption of normal muscular activity. In a previous study, we reported that recovery of bone mass after BtxA injection was incomplete 12 weeks post injection despite the return to normal ambulatory function after muscle function recovery (13). We also found an increase in marrow area and decrease in cortical thickness in bones after BtxA induced muscle paralysis (13).

Our present results indicate that trabecular bone loss occurs similarly in the mutant and wild type mice. However, osteoblast/osteocyte Cx43 deficient mice, whose cortical bone is thinner and bone marrow area larger relative to wild type mice, are less sensitive to the effect of skeletal unloading on the structural, cellular and biomechanical features of cortical bone, demonstrating that Cx43 deficiency in osteoblasts/osteocytes has complex and envelope-specific modulatory effects on bone response to mechanical loading. These results underscore an abnormal regulation of bone remodeling by Cx43 deficient osteoblasts and/or osteocytes, which are unable to produce normal adaptive responses to mechanical stimuli.

MATERIAL AND METHODS

Transgenic Mice

Mice harboring a floxed *Gja1* allele ($Gja1^{flox}$) were mated with mice expressing Cre under control of a 2.3 kb $\alpha_1(I)$ *collagen* promoter fragment (*ColCre*) so that Cre-mediated recombination replaces the entire *Gja1* reading frame with a *lacZ* reporter cassette, as described (5). Homozygous $Gja1^{flox/flox}$ mice were mated with *ColCre* mice also carrying a *Gja1* null allele ($ColCre;Gja1^{+/-}$) to generate in approximately equal numbers, $ColCre;Gja1^{-/flox}$ (conditional knockout, cKO), and $Gja1^{+/flox}$ (wild type equivalent, WT). Because of gender-specific differences in bone structure, these studies were performed only in male mice. All mouse lines were produced in a mixed C57BL/6-C129/J background. Mice were fed regular chow and housed communally in a room maintained at a constant temperature (25°C) on a 12 hours light/dark cycle. There are no significant differences in food intake between the WT and cKO mice (6). Genotyping and verification of Cre-mediated DNA recombination were performed as described (5,6). All procedures were approved by the Animal Studies Committee of Washington University in St. Louis and were

in accordance with the Public Health Service Policy on Humane Care and Use of Laboratory Animals.

Experimental Design and Procedures

A total of 20 WT and 20 cKO 4-month-old male mice were used in this study. For each genotype, 10 mice were injected with botulinum toxin A (BtxA), (Allergan Inc., Irvine CA) at the dose of 2 U/100 g body weight (12–15), and 10 were injected with an equal volume of saline (20μl). One half of the total volume was injected into the quadriceps muscle group and the other half into the triceps surae muscle group under isofluroane anesthesia. The contra-lateral limb was used as an internal control. Since the goals of the study were to determine the effect of acute muscle unloading and recovery, half of the mice in each genotype and treatment groups were sacrificed at 3 weeks post-injection, when bone loss following muscle paralysis reaches its nadir (12,13). The other half of the mice were left to recover muscle function and bone mass until week 19 post-injection when they were sacrificed (Figure 1A). The mice followed until week 3 were injected with calcein (15 mg/kg, ip; Sigma-Aldrich, St. Louis, MO) on days 12 and 19 post injection (BtxA or Saline) for dynamic histomorphometry. Mice followed until week 19 received their calcein injections on days 124 and 131 post BtxA or Saline injection. In either case, the second calcein dose was administered 2 days before sacrifice.

The degree of muscle paralysis was assessed daily over a 3-week period using the Digital Abduction Scoring (DAS) test (16), where the degree of abduction of the digits in the paralyzed limb are assessed and scored using a scale of 0 to 4, with 0 reflecting normal muscle function and 4 indicating total paralysis. We also measured muscle area monthly using in vivo micro-computed tomography (μCT, see below). For the mice sacrificed 3 weeks post injection, the injected and control hind limbs were dissected and weighed prior to the removal of soft tissue.

Post mortem, tibiae were cleaned of all soft tissue, fixed in 10% buffered formalin for up to 24 hours and then stored at 4°C in 70% ethanol before embedding for histological analysis. The femora were wrapped in PBS soaked gauze and kept frozen at −20°C until analysis. The ileum was cleaned, flash frozen in liquid nitrogen, and stored at −80°C until DNA extraction.

Bone Microstructure

In vivo analysis—For longitudinal analysis of bone microstructure and mineralization, animals were subjected to in vivo scanning using μCT (VIVA CT 40, Scanco Medical AG, Switzerland). The leg to be scanned was fully extended and isolated from the body, while the mouse snout was kept in a mask to ensure the continuous flow of isoflurane (1–2%) during the entire scan. To minimize the variability due to leg repositioning for repeat in vivo μCT scanning, we developed a fixture designed to orient the leg in a standard position. Scans included 100 slices encompassing the proximal epiphysis and metaphysis of the tibia, including the region of the growth plate, and 25 slices of the diaphysis 5 mm proximal to the tibia-fibular junction. These regions were scanned at 21.5 μm voxel resolution, 109μA current and 70 kEV. The metaphysis was analyzed for trabecular bone volume/tissue volume (BV/TV), trabecular number (Tb.N), separation (Tb.Sp) and thickness (Tb.Th), and tissue mineral density (TMD) - the volumetric density of the trabecular fraction. In the diaphyseal scans, marrow area (Ma.Ar), tissue area (Tt.Ar), cortical area (Ct.Ar = Cortical volume ÷ (no. slices × slice thickness)) and cortical BMD were determined. The cortical area fraction was determined as Ct.Ar/Tt.Ar (17). Tibial cortical thickness (Ct.Th) was determined as the average of measurements at 5 locations per bone from 3 different slices. The different locations were chosen to account for the irregular shape of the tibia. Muscle area was

determined by tracing the outline of the visible muscle and subtracting the area corresponding to tibia and fibula from 3 slices.

To minimize the effects of radiation exposure on BV/TV – an important consideration particularly in mice from a C57BL/6J background (18) – we limited μCT scanning to one every 3–4 weeks. Both injected and non-injected legs were scanned at each time-point, to account for any potential systemic effects of radiation and/or treatment.

Ex vivo analysis—Right and left femora were stabilized in 1.5–2.0% agarose gel and 4 regions (6 slices each) of the diaphysis were scanned ±0.5mm and ±1.5mm from the mid-diaphysis at 16-μm voxel resolution and 55KeV (μCT 40; Scanco Medical AG), as described previously(6). Second area moment of inertia (MOI) was calculated relative to the axis of bending (anterior-posterior). Mean Ct.Th. of the femur was determined manually from 4 measurements of width from 3 slices and taking the average value for each bone.

Bone Histomorphometry

Tibiae were embedded in methyl methacrylate using the method described previously (5,6). Longitudinal sections of the whole bone (4 μm thickness) were made as close to the center of the bone as possible and 3 sections per block were cut for triplicate measurements. Two of these were stained for tartrate resistant acid phosphatase (TRAP). One section per bone was left unstained for assessment of calcein fluorescence. Fluorescent images were obtained using a confocal microscope (LSM 510, Axiovert 200M, Plan-Neofluar 10X/0.30 NA Objective, Carl Zeiss, Jena, Germany). Quantitative histomorphometry was performed at the mid-diaphysis using commercial software (OSTEO II, Bioquant, Nashville, TN, USA), and separately for endocortical and periosteal surfaces, when appropriate. According to established nomenclature (19), osteoclast surface per bone surface (OcS/BS) and osteoclast number (OcN/BS) were determined from TRAP stained sections at the mid diaphysis. As an index of bone formation, mineralizing surface (MS/BS) was determined from calcein-labeled sections, as previously described (5). Because of the scarcity of double calcein labels in the mid diaphysis, mineral apposition rate or bone formation rate could not be reliably estimated (20).

Bone Biomechanics

Right and left femora were tested in three point bending to failure using methods previously described (21,22). Specimens were stabilized over two supports placed 7mm apart in an Instron 8841 apparatus (Instron, Norwood, MA). A loading force was applied in the anterior/posterior direction midway between the two supports by a displacement ramp at a rate of 0.03 mm/s. Force and displacement data were collected at 100 Hz (Labview 5.0, National Instruments, Austin, TX) and test curves were analyzed to determine ultimate force to failure and stiffness.

Statistical Analyses

Two-way analysis of variance (ANOVA) was used to assess differences for each genotype using treatment and time as the independent variables, after testing for normality and equality of variance. When the F value was significant, the Holm-Sidak post-hoc test was used for group comparisons at specific time points. Where appropriate, an unpaired Student t-test was used for group comparisons. Data were managed in Microsoft Excel and analyzed using the SigmaPlot 11.0 statistical package (Systat Software Inc., Chicago, Illinois). Group values are expressed as the mean ± sem, unless otherwise noted.

RESULTS

Consistent with previous reports (5,6), cKO mice weighed significantly less than WT mice at baseline (27.57±1.01 g vs. 30.33±1.79 g respectively, $p<0.05$). During the first week after BtxA injection there was about 4% weight loss in both genotypes, whereas injection of saline had no significant effect on body weight. By day 10 post-injection, all BtxA injected mice had regained their weight to pre-injection levels (Fig. S1A). As also anticipated from previous studies (12–15), BtxA injection caused rapid loss of muscle function with complete paralysis by 24 h post injection lasting for 4–5 days. A slow recovery of muscle function began thereafter and was complete by 3 weeks as indicated by the DAS scores (Fig. 1B). Parallel changes in muscle area in the BtxA-injected limb were observed, with a rapid decline approximating 40% of baseline within the first 3–7 weeks followed by a slow recovery, which was complete only after 19 weeks (Fig. 1C). Mice of both genotypes experienced an equal degree of muscle atrophy and recovered at similar rates; while no changes in muscle area occurred in the saline injected mice (Fig. 1C). There was a slow but non-significant trend towards a decrease in muscle mass in the contra-lateral limb of BtxA injected mice (Fig. S1B). Limbs were weighed in mice sacrificed 3 weeks after BtxA injection. Corroborating the imaging studies, BtxA injected limbs weighed significantly less than control limbs in both genotypes (1.64±0.15 g vs. 2.13±0.16 g for cKO; 1.70±0.17 g vs. 2.04±0.26 g for WT respectively, $p < 0.05$).

As previously shown (6), baseline BV/TV and cortical thickness were significantly lower in cKO mice relative to WT littermates, whereas marrow area and total tissue area were larger (Table 1). Cortical thickness and the percent of cortical area relative to total bone area were lower in cKO relative to WT (Table 1), thus confirming the larger but thinner cortical bone phenotype described in this and other *Gja1* mutant models (6,23). On the other hand, in this μCT analysis we did not see a lower trabecular thickness we had previously reported in histologic sections of cKO mice (5); this may be related to the different techniques used, which is reported to be particularly evident for trabecular thickness (24,25). Significant loss of trabecular bone mass occurred in the BtxA-injected limbs of both WT and cKO mice following muscle paralysis, and BV/TV reached a minimum at 3 weeks followed by a modest trend towards recovery (Fig. 2A). Importantly, there was also a slow but progressive decrease of BV/TV in the control, non-injected limb over the course of the study, though trabecular bone mass remained higher in the control limbs relative to BtxA-injected limbs at week 19 (Fig. 2A). No significant changes in BV/TV occurred in saline-injected WT or cKO mice (Fig. S1B). To control for this systemic bone loss in BtxA injected animals and determine the true effect of BtxA induced muscle paralysis on bone, data for the injected limb were normalized to the contra-lateral non-injected limb in each animal, and expressed as percent changes from baseline. Such normalized data represent the degree of imbalance between injected and non-injected limbs across time. Analysis of the normalized data revealed a rapid and profound bone loss in BtxA-injected limbs from both genotypes; BV/TV reached a nadir of about 30–40% below baseline at 3 weeks, followed by an apparent recovery phase. Such recovery was only partial since at 19 weeks BV/TV of the BtxA-injected limbs was still >10% lower relative to their controls (Fig. 2B). The patterns of rapid bone loss and slow recovery were similar in WT and cKO mice, even though the recovery was slightly delayed in the latter. No significant bone loss was observed in the limbs injected with saline throughout the study (Figure 2B, S1C). The magnitude of trabecular bone loss 3 weeks after intramuscular BtxA injection is exemplified in the 3D reconstruction of the femoral proximal epiphyses by μCT (Figs. 2C and D). At 19 weeks the trabecular structure was quite similar to week 3 for both WT and cKO.

Analysis of structural parameters by μCT revealed a sharp decrease in trabecular thickness at 3 weeks post-injection in both BtxA treated groups, a difference that resolved with time in

WT but only partially in cKO mice (Table 2). Trabecular number also decreased but more slowly and not as profoundly, and it also recovered at the end of the study in both genotypes (Table 3). In parallel, trabecular separation increased and tissue mineral density sharply declined in both BtxA-injected groups, and these differences became non-significant at the end of the study (Tables S1 and S2). We did not detect any genotype effect on any of these changes. Thus, muscle paralysis induced a loss of trabecular bone that is accounted for by a rapid trabecular thinning followed by loss of trabecular number, and is largely independent of Cx43.

Data on cortical bone parameters were also normalized to the contra-lateral, non-injected limb in each animal, and expressed as percent changes from baseline. Accordingly, there was a sharp, significant increase in marrow area in the BtxA injected limb of WT mice 3 weeks post-injection, whereas only a very modest and transient increase was observed in the cKO bones (Fig. 3A). After 3 weeks, the difference between BtxA-injected and control limb remained stable, with a tendency to recover at 15 weeks. There was a significant genotype effect in the two-way ANOVA. On the contrary, no imbalance between injected and control limbs were detected in the saline groups of either genotype (Fig. 3A; Fig S2A). Parallel and reciprocal changes in cortical area occurred in WT animals, with a significant decrease in the BtxA injected limbs relative to the control limbs 3 weeks post-injection, followed by a modest trend to recovery thereafter, contrasting with non-significant changes in the cKO mice (Fig. 3B). Again, there was a significant genotype effect on the BtxA-treated groups, whereas no such effect was seen for saline injected mice. No significant changes in these cortical parameters were detected in the control limb of either genotype (Fig. S2A–C). We observed no significant imbalances in total tissue area or cortical BMD after BtxA injection in WT or cKO mice (Tables S3, S4), suggesting that the effects of muscle paralysis on cortical bone occur primarily at the endocortical surface. Interestingly, cortical area fraction in the WT decreased after BtxA injection towards levels similar to cKO mice, followed by partial recovery at 19 weeks (Figure S2C). The rapid expansion of the marrow cavity in the WT mice was evident 3 weeks post BtxA injection (Fig. 3C upper panel), and did not appear to change further up to 19 weeks post BtxA injection. By contrast, tibia of cKO, whose marrow cavity is already larger compared to WT littermates (Table 1), did not exhibit any substantial changes after BtxA injection for the duration of the study (Fig. 3C, lower panels; Fig. S2B).

Bone histomorphometric analyses of the endocortical surface of tibiae from mice sacrificed 3 weeks after the injections revealed a significant increase in osteoclast number and osteoclast surface in BtxA-injected limbs relative to control limbs in WT mice, an effect that was not statistically significant in cKO mice (Fig. 4A, B). The relative increases in osteoclast number and osteoclast surface were significantly different between WT and cKO ($p=0.049$ and $p=0.043$, respectively; two-tailed t-test). In absolute terms, osteoclast number and surface were higher in control cKO relative to WT mice (Fig. S3A-D), as expected from a previous study (23), and there were no effects of saline (Fig. S3A, C). However, osteoclast number and surface increased 4-fold after BtxA injection in WT mice, while no changes occurred in cKO mice (Fig. S3B, D).

At 3 weeks post-injection, bone formation assessed as mineralizing surface was similar across all treatment and genotype groups on the endosteal side at the mid-diaphysis (Fig. 4C). Mineralizing surface on the periosteal side was tendentially higher in BtxA injected limbs relative to control limbs, particularly in cKO mice, but these differences did not reach statistical significance (Fig. 4D). In mice sacrificed after 19 weeks, we found very few osteoclasts on the endocortical surfaces and no differences between injected and control legs, regardless of treatment or genotype (not shown). Likewise, there were no differences in bone mineralizing surface at either the endocortical or periosteal surfaces in any groups (Fig.

S3B, C). These results are consistent with no changes in cortical thickness and tissue area even after 19 weeks post BtxA injection. Since we found no differences between cKO and WT in the trabecular bone as a consequence to BtxA injection, we did not perform dynamic histomorphometry in the trabecular envelope.

We then tested the consequences of BtxA injection on cortical bone biomechanical properties. By examining the bones from non-injected legs, we confirmed that the geometric moment of inertia is higher and that ultimate force and stiffness are significantly lower in cKO than in WT mice (Fig. S4A, B, C), as we had reported earlier (6). Therefore to assess the effect of BtxA, we applied the same normalization method as described above for the structural parameters. Accordingly, the calculated geometric moment of inertia was significantly different in WT BtxA-injected limbs relative to their contra-lateral controls 3 weeks after the injection (Fig. 5A), relative to saline-injected limbs, but it did increase after 19 weeks in the cKO group (Fig. 5B). There were no differences between injected and control limbs in the saline groups. On the other hand, we detected a significant decrease in ultimate force to failure 3 weeks after BtxA injection in both WT and cKO mice, although the magnitude of this effect was about 40% lower in the cKO mice (Fig. 5C). Such imbalance between BtxA-injected and control limbs did not persist at week 19 (Fig. 5D), and it was not evident at any time-points in the groups injected with saline. Similarly, we observed a significant decrease in stiffness in the WT BtxA-injected relative to control leg 3 weeks after injection but not in the cKO mice (Fig. 5E). By week 19, a treatment-related imbalance in stiffness was detected in the cKO, even though a greater variability within each group was noted (Fig. 5F). We detected no significant changes in cortical BMD of the tibia (Table S4), however in WT mice injected with BtxA there was significant cortical thinning (Table 4).

DISCUSSION

Muscle paralysis produced by BtxA injection in hind limb muscles results in rapid and significant loss of trabecular bone mass, expansion of bone marrow cavity with cortical thinning, and deteriorating bone strength, abnormalities attended by activation of endocortical bone resorption. These changes are not reversed 19 weeks after BtxA injection, despite a reversal of bone remodeling towards increased bone formation upon recovery of muscle function. Lack of Cx43 in osteoblasts and osteocytes does not affect trabecular bone loss but it attenuates the effects of muscle paralysis on cortical bone structure and strength. Our study indicates that lack of Cx43 in osteoblasts and osteocytes results in a cortical bone phenotype similar to WT bones subjected to skeletal muscle unloading.

We had previously reported rapid bone loss following a single BtxA injection in limbs using dual energy X-ray absorptiometry, which includes all bones in a limb (13). Using in vivo μCT, others have recently reported trabecular bone loss and decreased cortical thickness with increased endocortical volume but without changes in periosteal volume following transient muscle paralysis (14), findings very consistent with our results in WT mice. In this study, we also show that these changes are indeed related to a rapid activation of endocortical bone resorption following muscle paralysis, and result in a rapid and significant deterioration of the bone biomechanical properties in the BtxA injected limbs. The reason for the selective attenuation of this effect on cortical bone by Cx43 deficiency is not immediately obvious. It is conceivable that the already higher endocortical osteoclast number in cKO mice at baseline may by itself limit further osteoclast activation by mechanical unloading. Alternatively, less efficient gene recombination in trabecular osteoblasts, as we have recently observed using a different promoter to drive *Gja1* ablation (23), may contribute to explain the lack of a Cx43 effect on the trabecular envelope. However, in the model used in this study we did detect effective *Gja1* deletion in cancellous

bone (5). Notably, data from another group (unpublished) also suggest that the action of Cx43 on adult bone occurs primarily on the cortical envelope with minimal effects on the trabecular compartment (26). There were no differences in the patterns of muscle function (and mass) loss and recovery between WT and cKO mice; nor was there any evidence of significant changes in muscle area in control limbs during the study to indicate either atrophy (because of a possible systemic effect of BtxA) or hypertrophy (thus excluding a compensatory muscle overloading in the contra-lateral limbs). Furthermore, we observed no differences in cage activity between genotypes, and changes in body weight were also similar, indicating that the two genotype groups were exposed to similar loading patterns from muscular contraction and gravity. Therefore, the attenuated response of cortical bone to transient muscle paralysis in cKO mice strongly suggest that Cx43 in osteoblasts and/or osteocytes is crucially involved in elaborating the signals generated by muscle contraction into biologic effect on cortical bone remodeling.

Since *Gja1* deletion in our model is restricted to cells of the osteoblast lineage in later stages of differentiation (5), the modulatory effect of Cx43 of endocortical osteoclasts must be indirect, via the osteoblast or the osteocyte. In fact, we have recently demonstrated that one of the consequences of *Gja1* ablation in the osteogenic lineage is increased support of osteoclastogenesis (23). Intriguingly, a similar phenotype with widened and thinner long bones and resistance to unloading-induced bone loss was reported in mice with targeted ablation of osteocytes (27), raising the possibility that loss of muscle action on bone may down-regulate a Cx43-dependent anti-osteoclastogenic signal from osteocytes. It is worth noting that the cortical compartment of long bones of Cx43-deficient mice is structurally, metabolically and biomechanically very similar to WT bones subjected to acute skeletal muscle unloading. Such phenotype is also similar to that seen in aging bone and in skeletal disuse (7–10,28). It is tempting to speculate that the abnormal cortical bone structure of Cx43 deficient animals may be the consequence of an altered response of osteoblasts and/or osteocytes to mechanical signals in the absence of Cx43. In other words, the cKO bones may perceive normal ambulatory loads as a disuse scenario, resulting in an abnormal up-regulation of endocortical resorption. In support of this hypothesis is the observation that the cortical phenotype develops after birth (23), and it thus represents an abnormality of adaptive responses to environmental factors. Based on in vitro studies, Cx43 may modulate mechanoresponsinevess in different, non-mutually exclusive ways: direct mechano-sensing in osteocytes (29), transmission of mechanically generated signals from osteocytes to osteoblasts (30), or modulation of osteoblast secretory activity (31). Further studies will examine these potential mechanisms.

In this study, neither the trabecular bone loss nor the cortical expansion was reversed 19 weeks after BtxA injection, despite a full recovery of muscle function. Thus, resolution of the imbalance in trabecular bone mass between BtxA and control limbs observed by 19 weeks post-injection does not represent a true “recovery” of bone mass, but it is the result of bone loss in the control bones relative to BtxA treated bones during the recovery period. On the other hand, trabecular bone loss in non-injected limbs may be related to the stress caused by the paralysis or to a systemic effect of the BtxA injection. Effects of BtxA at distant sites after intramuscular injection have been reported (32), but a recent study demonstrated that any non-muscle related effects of BtxA on bone is likely to be small or negligible compared to the effect on muscle function (33). This view is corroborated by our own unpublished in vitro studies showing no evidence of BtxA effects on either osteoblast cells or on osteoclastogenesis at doses relevant to those used in this in vivo study (data not shown). In any case, recovery from trabecular bone loss is only partial, as also shown by others (14), despite the fact that osteoclast number is no longer increased in the injected limbs after 19 weeks. While regaining of mechanical load by recovered muscle function rapidly reverses activation of bone resorption, bone formation is only modestly activated, and more on the

periosteal than on the endosteal surface. However, increased periosteal bone formation, already seen 3 weeks after induction of paralysis, is clearly not sufficient to reverse the structural changes caused by loss of muscle function. Likewise, although the imbalance in biomechanical parameters between injected and control limbs are resolved by week 19, WT bones do not recover their full bone strength. In this case, our results differ from those of Poliachik et al. (14), who instead observed full recovery of the cortical changes at 12 weeks. The reason for this discrepancy is unclear, although that report used female mice, whereas we used males, and it did not include data on control, non-injected limbs or bone biomechanics data. As noted, cKO mice are partially resistant to the cortical bone changes induced by BtxA injection, and no imbalance between injected and control bones was observed at the end of the study. The modest increase in periosteal bone formation in the BtxA-injected limb observed at 3 weeks did not carry through the end of the study, and was not sufficient to alter the cortical structure of cKO bones.

In conclusion, the results of this study demonstrate a significant role for Cx43 in the response of bone to mechanical unloading and reloading in the cortical envelope. Thus, Cx43 is required for full activation of endocortical bone resorption and expansion of the medullary cavity that follow muscle paralysis. Although long-term inhibition of Cx43 may lead to similar changes in cortical bone structure and strength, Cx43 may represent a target for short-term countermeasures for preventing the deterioration of bone structure and function in disuse osteoporosis.

Supplementary Material

Refer to Web version on PubMed Central for supplementary material.

Acknowledgments

This work was supported by NIH/NIAMS grants AR041255(RC), AR047867(MJS), P30AR057235 (Washington University Core Center for Musculoskeletal Biology and Medicine) and P30 DC004665 (Washington University Research Center for Auditory and Vestibular Studies Histology Core). Animals were housed in a facility supported by NIH Grant NCRR C06 RR015502.

References

1. Lecanda F, Warlow PM, Sheikh S, Furlan F, Steinberg TH, Civitelli R. Connexin43 deficiency causes delayed ossification, craniofacial abnormalities, and osteoblast dysfunction. J Cell Biol. 2000; 151(4):931–944. [PubMed: 11076975]
2. Paznekas WA, Boyadjiev SA, Shapiro RE, Daniels O, Wollnik B, Keegan CE, Innis JW, Dinulos MB, Christian C, Hannibal MC, Jabs EW. Connexin 43 (GJA1) mutations cause the pleiotropic phenotype of oculodentodigital dysplasia. Am J Hum Genet. 2003; 72(2):408–418. [PubMed: 12457340]
3. Kjaer KW, Hansen L, Eiberg H, Leicht P, Opitz JM, Tommerup N. Novel Connexin 43 (GJA1) mutation causes oculo-dento-digital dysplasia with curly hair. Am J Med Genet. 2004; 127A(2): 152–157. [PubMed: 15108203]
4. Flenniken AM, Osborne LR, Anderson N, Ciliberti N, Fleming C, Gittens JE, Gong XQ, Kelsey LB, Lounsbury C, Moreno L, Nieman BJ, Peterson K, Qu D, Roscoe W, Shao Q, Tong D, Veitch GI, Voronina I, Vukobradovic I, Wood GA, Zhu Y, Zirngibl RA, Aubin JE, Bai D, Bruneau BG, Grynpas M, Henderson JE, Henkelman RM, McKerlie C, Sled JG, Stanford WL, Laird DW, Kidder GM, Adamson SL, Rossant J. A Gja1 missense mutation in a mouse model of oculodentodigital dysplasia. Development. 2005; 132(19):4375–4386. [PubMed: 16155213]
5. Chung DJ, Castro CH, Watkins M, Stains JP, Chung MY, Szejnfeld VL, Willecke K, Theis M, Civitelli R. Low peak bone mass and attenuated anabolic response to parathyroid hormone in mice with an osteoblast-specific deletion of connexin43. J Cell Sci. 2006; 119(Pt 20):4187–98. [PubMed: 16984976]

6. Grimston SK, Brodt MD, Silva MJ, Civitelli R. Attenuated response to in vivo mechanical loading in mice with conditional osteoblast ablation of the connexin43 gene (Gja1). J Bone Miner Res. 2008; 23(6):879–86. [PubMed: 18282131]
7. Maggio D, Pacifici R, Cherubini A, Simonelli G, Luchetti M, Aisa MC, Cucinotta D, Adami S, Senin U. Age-related cortical bone loss at the metacarpal. Calcif Tissue Int. 1997; 60(1):94–7. [PubMed: 9030488]
8. Dequeker J. Bone and ageing. Ann Rheum Dis. 1975; 34(1):100–15. [PubMed: 164839]
9. Weinreb M, Rodan GA, Thompson DD. Osteopenia in the immobilized rat hind limb is associated with increased bone resorption and decreased bone formation. Bone. 1989; 10(3):187–194. [PubMed: 2803854]
10. Jee WS, Ma Y. Animal models of immobilization osteopenia. Morphologie. 1999; 83(261):25–34. [PubMed: 10546233]
11. Chappard D, Chennebault A, Moreau M, Legrand E, Audran M, Basle MF. Texture analysis of X-ray radiographs is a more reliable descriptor of bone loss than mineral content in a rat model of localized disuse induced by the Clostridium botulinum toxin. Bone. 2001; 28(1):72–9. [PubMed: 11165945]
12. Warner SE, Sanford DA, Becker BA, Bain SD, Srinivasan S, Gross TS. Botox induced muscle paralysis rapidly degrades bone. Bone. 2006; 38(2):257–264. [PubMed: 16185943]
13. Grimston SK, Silva MJ, Civitelli R. Bone loss after temporarily induced muscle paralysis by Botox is not fully recovered after 12 weeks. Ann NY Acad Sci. 2007; 1116:444–460. [PubMed: 17584988]
14. Poliachik SL, Bain SD, Threet D, Huber P, Gross TS. Transient muscle paralysis disrupts bone homeostasis by rapid degradation of bone morphology. Bone. 2010; 46(1):18–23. [PubMed: 19857614]
15. Manske SL, Boyd SK, Zernicke RF. Muscle and bone follow similar temporal patterns of recovery from muscle-induced disuse due to botulinum toxin injection. Bone. 2010; 46(1):24–31. [PubMed: 19853070]
16. Aoki KR. A comparison of the safety margins of botulinum neurotoxin serotypes A, B, and F in mice. Toxicon. 2001; 39(12):1815–20. [PubMed: 11600142]
17. Bouxsein ML, Boyd SK, Christiansen BA, Guldberg RE, Jepsen KJ, Muller R. Guidelines for assessment of bone microstructure in rodents using micro-computed tomography. J Bone Miner Res. 25(7):1468–86. [PubMed: 20533309]
18. Klinck RJ, Campbell GM, Boyd SK. Radiation effects on bone architecture in mice and rats resulting from in vivo micro-computed tomography scanning. Med Eng Phys. 2008; 30(7):888–95. [PubMed: 18249025]
19. Parfitt AM, Drezner MK, Glorieux FH, Kanis JA, Malluche H, Meunier PJ, Ott SM, Recker RR. Bone histomorphometry: standardization of nomenclature, symbols, and units. Report of the ASBMR Histomorphometry Nomenclature Committee. J Bone Miner Res. 1987; 2(6):595–610. [PubMed: 3455637]
20. Foldes J, Shih MS, Parfitt AM. Frequency distributions of tetracycline-based measurements: implications for the interpretation of bone formation indices in the absence of double-labeled surfaces. J Bone Miner Res. 1990; 5(10):1063–7. [PubMed: 2080717]
21. Di Benedetto A, Watkins M, Grimston SK, Salazar VS, Donsante C, Mbalaviele G, Radice G, Civitelli R. N-cadherin and caderin 11 modulate postnatal bone growth and osteoblast differentiation by distinct mechanisms. J Cell Biol. 2010:123. (In press).
22. Willinghamm MD, Brodt MD, Lee KL, Stephens AL, Ye J, Silva MJ. Age-related changes in bone structure and strength in female and male BALB/c mice. Calcif Tissue Int. 86(6):470–83. [PubMed: 20405109]
23. Watkins M, Grimston SK, Norris JY, Guillotin B, Shaw A, Beniash E, Civitelli R. Osteoblast connexin43 modulates skeletal architecture by regulating both arms of bone remodeling. Mol Biol Cell. 2011; 22(8):1240–1251. [PubMed: 21346198]
24. Chappard D, Retailleau-Gaborit N, Legrand E, Basle MF, Audran M. Comparison insight bone measurements by histomorphometry and microCT. J Bone Miner Res. 2005; 20(7):1177–84. [PubMed: 15940370]

25. Muller R, Van Campenhout H, Van Damme B, Van Der Perre G, Dequeker J, Hildebrand T, Ruegsegger P. Morphometric analysis of human bone biopsies: a quantitative structural comparison of histological sections and micro-computed tomography. Bone. 1998; 23(1):59–66. [PubMed: 9662131]

26. Bivi, N.; Aguirre, JI.; Vyas, K.; Allen, M.; Bellido, T.; Plotkin, L. Increased osteocyte apoptosis and bone resorption, and decreased strength of cortical but not trabecular bone in mice lacking connexin43 in osteoblasts and osteocytes. J Bone Miner Res. 2009. Avaialble at http://www.asbmr.org/Meetings/AnnualMeeting/AbstractDetail.aspx?aid=77a3ec41-fa04-4fec-95f2-a032eea3e807

27. Tatsumi S, Ishii K, Amizuka N, Li M, Kobayashi T, Kohno K, Ito M, Takeshita S, Ikeda K. Targeted ablation of osteocytes induces osteoporosis with defective mechanotransduction. Cell Metab. 2007; 5(6):464–75. [PubMed: 17550781]

28. Ruff CB, Hayes WC. Subperiosteal expansion and cortical remodeling of the human femur and tibia with aging. Science. 1982; 217(4563):945–8. [PubMed: 7112107]

29. Cherian PP, Siller-Jackson AJ, Gu S, Wang X, Bonewald LF, Sprague E, Jiang JX. Mechanical strain opens connexin 43 hemichannels in osteocytes: a novel mechanism for the release of prostaglandin. Mol Biol Cell. 2005; 16(7):3100–3106. [PubMed: 15843434]

30. Genetos DC, Kephart CJ, Zhang Y, Yellowley CE, Donahue HJ. Oscillating fluid flow activation of gap junction hemichannels induces ATP release from MLO-Y4 osteocytes. J Cell Physiol. 2007; 212(1):207–14. [PubMed: 17301958]

31. Stains JP, Civitelli R. Gap junctions regulate extracellular signal-regulated kinase signaling to affect gene transcription. Mol Biol Cell. 2005; 16(1):64–72. [PubMed: 15525679]

32. Curra A, Berardelli A. Do the unintended actions of botulinum toxin at distant sites have clinical implications? Neurology. 2009; 72(12):1095–9. [PubMed: 19307544]

33. Manske SL, Boyd SK, Zernicke RF. Muscle changes can account for bone loss after botulinum toxin injection. Calcif Tissue Int. 2010; 87(6):541–9. [PubMed: 20967431]

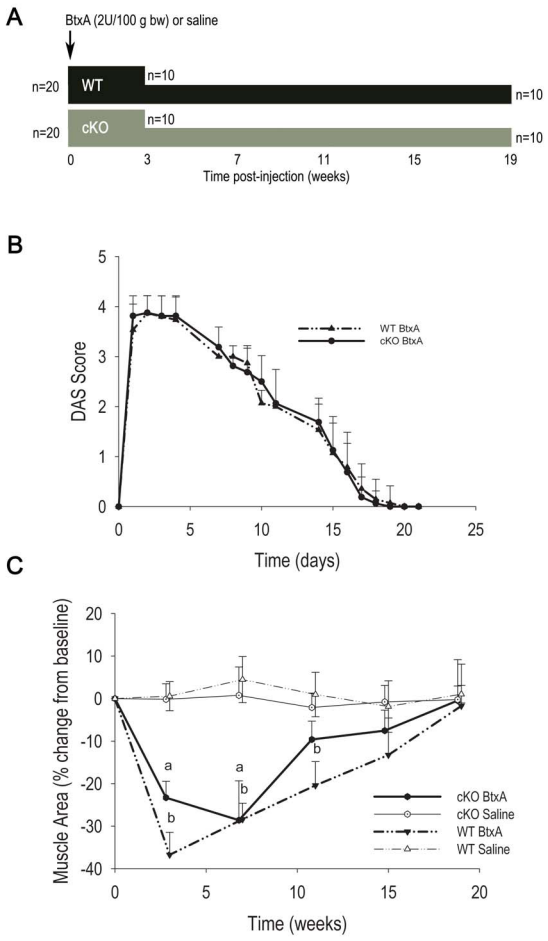

Figure 1.

Study design and effect of BtxA injection on muscle function and mass. **A.** Diagrammatic representation of the study design. A total of 40 mice were used, 20 of each genotype. Twenty mice were sacrificed 3 weeks after intramuscular injection of botulinum toxin A (BtxA) or saline (5 per treatment for each genotype); and 20 were followed up to 19 weeks (5 per treatment for each genotype). The mice followed for 19 weeks had in vivo μCT scans every 4 weeks. **B.** Changes in muscle function assessed by Digital Abduction Score (DAS) after BtxA injection. Muscle paralysis (DAS=4) and recovery were similar in wild type (WT) and conditional knockout (cKO). **C.** Change in muscle area measured by μCT in WT and cKO mice followed for 19 weeks. There was a significant effect of treatment on muscle area by 2-way ANOVA ($p<0.05$); $p < 0.05$. a: $p < 0.05$ vs cKO Saline; b: $p < 0.05$ vs WT Saline.

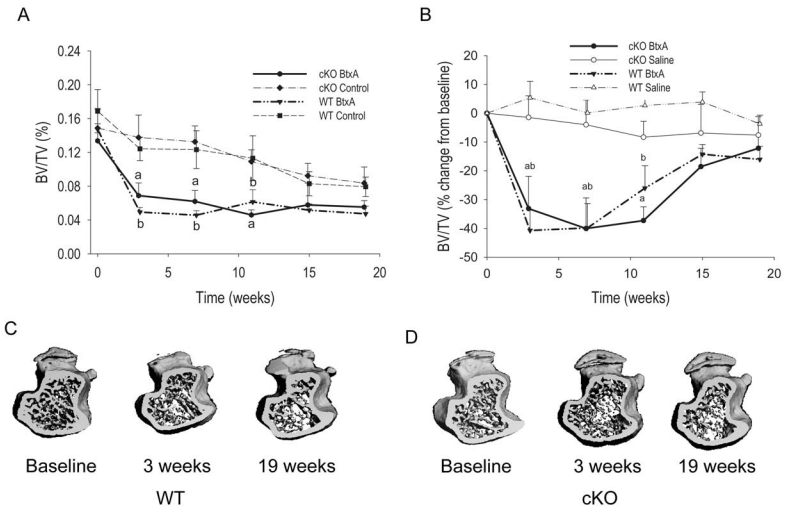

Figure 2.

Effect of botulinum toxin A (BtxA) on trabecular bone in wild type (WT) and *Gja1* conditional knockout (cKO) mice. **A.** Trabecular bone volume (BV/TV) in injected (BtxA) and control limbs of mice followed for 19 weeks. There was a significant decrease of BV/TV in the tibiae in the BtxA injected limbs compared with control tibiae. a: $p < 0.05$ vs cKO BtxA Control; b: $p < 0.05$ vs WT BtxA Control. **B.** Difference in BV/TV between injected (BtxA or saline) and non-injected control limbs, expressed as a percentage of baseline. Following the injection, the difference (imbalance) between injected and non-injected limbs sharply decreased selectively in the BtxA but not in the saline groups of each genotype. There is a progressive though incomplete recovery thereafter. There was a significant effect of treatment and time ($p<0.05$) but no effect of genotype by 2-way ANOVA. a: $p < 0.05$ vs cKO Saline; b: $p < 0.05$ vs WT Saline. **C.** Micro-CT generated 3-D reconstruction of metaphyses of WT BtxA and (**D**) tibiae of cKO BtxA injected limbs at different time-points.

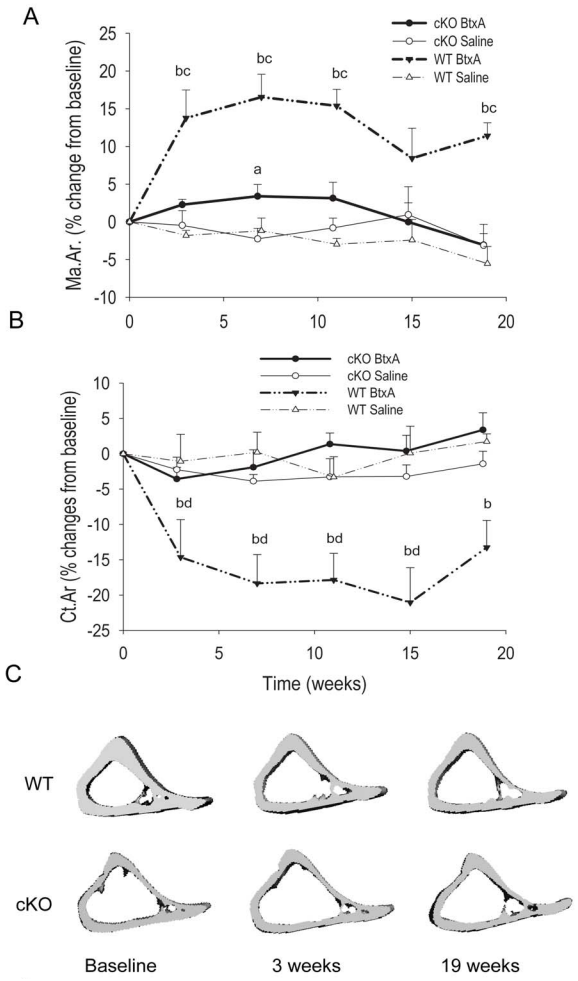

Figure 3.

Effect of botulinum toxin A (BtxA) on cortical bone in wild type (WT) and *Gja1* conditional knockout (cKO). **A**. Difference in Marrow Area (Ma.Ar.) between injected (BtxA or saline) and non-injected control limbs, expressed as a percentage of baseline. There was significant expansion of the marrow cavity for WT mice beginning 3 weeks post BtxA injection and persisting through the 19 weeks of the study. There was a significant effect of genotype and treatment by 2-way ANOVA ($p < 0.05$). **B.** Difference in Cortical Area (Ct.Ar) between injected (BtxA or saline) and non-injected control limbs, expressed as a percentage of baseline. There was a significant reduction in relative cortical area over time for the WT BtxA mice. There was a significant genotype effect in the BtxA group ($p<0.05$) but not in the Saline mice by 2-way ANOVA ($p>0.05$). No significant changes in Ct.Ar were observed for the cKO BtxA mice over the 19 weeks of the study. **C.** Micro-CT generated 3-D reconstruction of diaphyses of WT and cKO taken at baseline, 3 weeks and 19 weeks for each genotype. a: $p < 0.05$ vs cKO Saline, b: $p < 0.05$ vs WT Saline, c: $p < 0.05$ vs cKO BtxA, d: $p < 0.05$ vs WT Baseline.

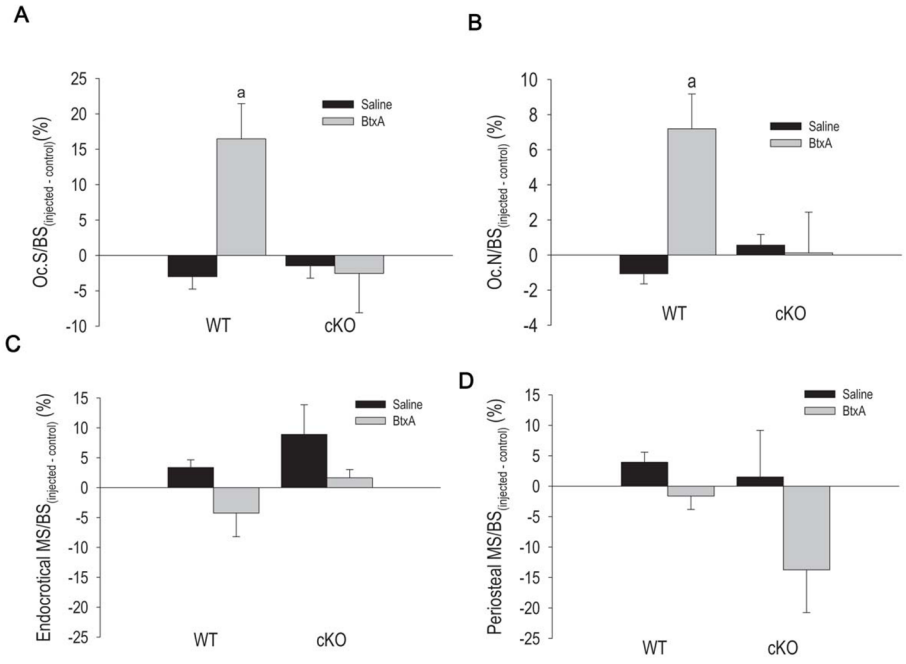

Figure 4.

The effect of botulinum toxin A (BtxA) on in wild type (WT) and *Gja1* conditional knockout (cKO) mice on parameters of bone resorption as determined via TRAP staining for osteoclasts at the mid diaphysis (n=12 per genotype group), and measures of bone formation as determined via calcein labeling. Results are expressed as the absolute difference from the Control limb. **A.** osteoclast surface/bone surface (OcS/BS) for mice sacrificed 3 weeks after BtxA injection. a: $p < 0.05$ vs WT Saline. **B.** Number of osteoclasts per BS (N. Oc./BS) for mice sacrificed 3 weeks after BtxA injection. a: $p < 0.05$ vs WT Saline. **C.** Mineralizing surface/bone surface (MS/BS) at the endocortical surface of the mid-diaphysis in mice sacrificed 3 weeks post BtxA injection. **D.** Mineralizing surface/bone surface (MS/BS) at the periosteal surface of the mid diaphysis. There were no significant differences in terms of mineralizing surface between groups.

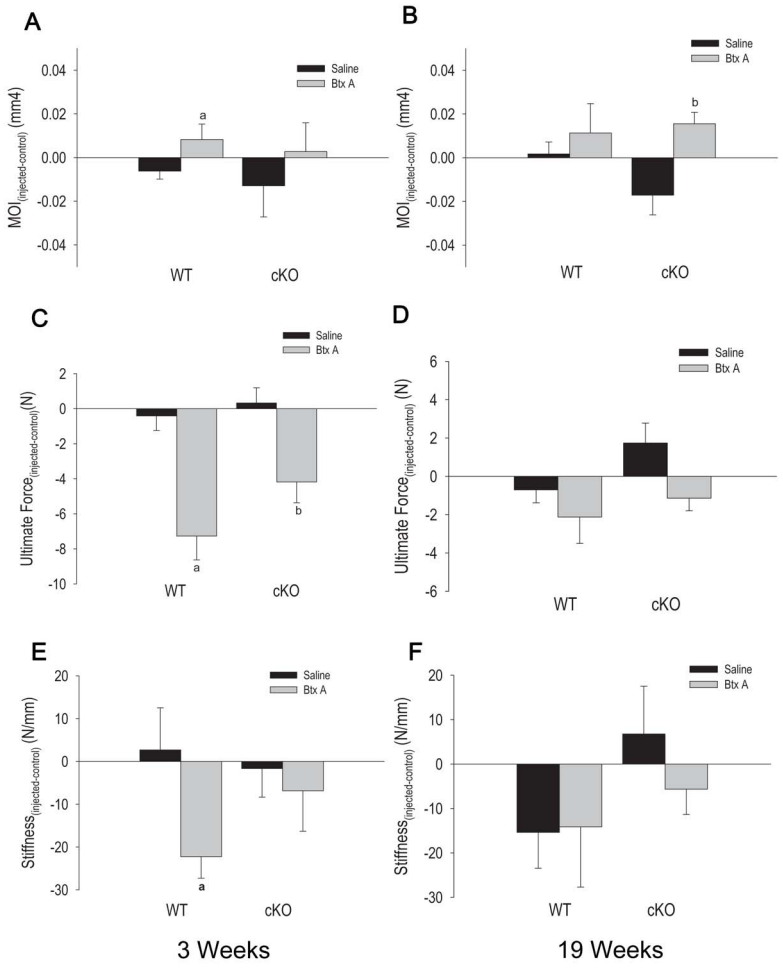

Figure 5.

Effect of Botulinum toxin A (BtxA) on biomechanical parameters at the mid diaphysis for wild type (WT) and *Gja1* conditional knockout (cKO) three weeks post injection and 19 weeks post injection. Results are expressed as the absolute change from the control limb of each group. **A.** Second area moment of inertia (MOI) values from mice sacrificed 3 weeks post-injection. a: $p < 0.05$ versus WT Saline. **B.** Second area moment of inertia (MOI) for WT and cKO, sacrificed 19 weeks post injection. b: $p < 0.05$ vs WT Saline. **C.** Ultimate Force (bone strength) data for mice sacrificed 3 weeks after BtxA injection. a: $p < 0.05$ vs WT Saline. **D.** Ultimate force (bone strength) data for mice sacrificed 19 weeks post-injection for WT and cKO mice. There were no significant differences in ultimate force between the BtxA and Saline groups at this later time point. **E.** Bone stiffness results for WT and cKO mice three weeks post BtxA injection. a: $p < 0.05$ versus WT Saline; **F.** Bone stiffness results for WT and cKO mice sacrificed after 19 weeks. b: $p < 0.05$ vs cKO Saline.

Table 1

Baseline Structural Parameters of Trabecular and Cortical Bone in wild type (WT) and Osteoblast/Osteocyte Conditional *Gja1* Knockout (cKO) Mice

	WT	cKO
BV/TV (%)	17.03±5.76	14.60±4.56*
Trabecular Number	5.35±0.69	5.21±0.75
Trabecular Thickness (mm)	0.56±0.05	0.56±0.09
Trabecular Separation (mm)	1.99±0.28	1.93±0.30
TMD (mgHA/cc)	163.71±39.71	154.65±36.97
Marrow Area (mm^2)	0.69±0.09	1.17±0.13*
Total Area (mm^2)	1.58±0.16	2.07±0.21*
Cortical Area (mm^2)	0.55±0.07	0.54±0.08
Cortical/Total Area(%)	34.89±2.57	26.53±2.69*
Cortical Thickness (mm)	0.184±0.017	0.157±0.022*

N=20 for each genotype.

* $p<0.05$ vs. WT, t-test for unpaired sample.

Table 2

Changes in Trabecular Thickness (percent of baseline) in BtxA or Saline Injected Limbs Relative to Non-Injected Control Limbs

Weeks since Injection	3	7	11	15	19
WT Saline	2.07±2.41	4.63±1.98	2.63±4.74	3.81±3.91	8.21±10.81
WT BtxA*	−22.66±6.92[b]	−6.67±6.17	−0.16±2.36	−0.52±4.04	−0.09±5.27
cKO Saline	0.13±3.14	−1.66±3.29	−0.47±2.37	−3.84±2.05	−3.49±1.76
cKO BtxA*	−24.63±7.98[a]	−9.67±3.12	−12.87±7.76	−11.72±3.91[c]	−9.71±6.65

WT: wild type mice; cKO: osteoblast/osteocyte conditional *Gja1* knockout mice

* significant effect of treatment (two way ANOVA);

[a] $p < 0.05$ vs. cKO Saline;

[b] $p < 0.05$ vs. WT Saline;

[c] $p < 0.05$ vs WT BtxA

Table 3

Changes in Trabecular Number (percent of baseline) in BtxA or Saline Injected Limbs Relative to Non-Injected Control Limbs

Weeks since Injection	3	7	11	15	19
WT Saline	1.51±3.55	2.49±3.89	1.91±3.21	2.68±3.32	1.75±4.18
WT BtxA*	−5.83±5.48	−5.45±5.69	−13.45±4.86^{b}	−7.42±3.77^{b}	−1.33±2.68
cKO Saline	−1.01±7.88	1.98±5.89	−0.75±6.31	1.60±3.72	1.40±10.69
cKO BtxA*	0.73±4.87	−9.36±3.10	−7.95±4.66	−4.98±4.99^{a}	0.01±3.95

WT: wild type mice; cKO: osteoblast/osteocyte conditional *Gja1* knockout mice

* significant effect of treatment (two way ANOVA);

^{a} $p < 0.05$ vs. cKO Saline;

^{b} $p < 0.05$ vs. WT Saline.

Table 4

Changes in Cortical Thickness (percent of baseline) in BtxA or Saline Injected Limbs Relative to Non-Injected Control Limbs

Weeks since Injection	3	7	11	15	19
WT Saline	5.09±4.09	−0.58±4.34	−0.11±4.87	6.64±4.63	3.19±3.49
WT BtxA*	−15.03±1.88^{ab}	−10.42±4.91	−14.44±2.42^{a}	−9.02±4.15	−5.28±5.23
cKO Saline	3.32±1.99	5.01±3.11	6.83±5.55	6.72±6.52	9.17±5.27
cKO BtxA*	−3.86±4.87	−4.07±3.25	−4.12±3.04	1.02±5.51	3.63±3.21

WT: wild type mice; cKO: osteoblast/osteocyte conditional *Gja1* knockout mice

*significant effect of treatment (two way ANOVA);

^{a} $p < 0.05$ vs. cKO Saline;

^{b} $p < 0.05$ vs. WT Saline.